

# Suitability of Widely Followed Earthquake Early Warning Systems to Seismically Active Regions of India, by Considering Destructive Intensity as a Parameter

Baro Olympa<sup>1</sup>, Kumar Ashok<sup>2</sup> and Kumar Abhishek<sup>3\*</sup>

<sup>1</sup> Civil Engineering, Kaziranga University, Assam, India

<sup>2</sup> Department of Earthquake Engineering, Indian Institute of Technology Roorkee, Uttaranchal, India

<sup>3</sup> Department of Civil Engineering, Indian Institute of Technology Guwahati, Assam, India  
Email: olympabaro@gmail.com, akmeqfeq@iitr.ac.in, abhiak@iitg.ac.in / abhitoaashu@gmail.com

**Abstract.** *Background:* Indian subcontinent has been witnessing moderate to damaging earthquakes (EQs) since prehistoric times. With growth in the population density and the construction activity, the probable damage during future EQs will also be manifold in comparison to the past. Issuing warnings in advance to the actual arrival of damage causing secondary waves under Earthquake Early Warning (EEW) system is widely followed in different parts of the globe. Though India has been facing EQ induced damages on an alarming level, no functioning EEW system is available in the Indian subcontinent. Present work tests the effectiveness of widely followed Compact Urgent Earthquake Detection and Alarm System (UrEDAS) of Japan by using Destructive Intensity (DI) as a parameter.

*Main findings:* To do so, firstly based on PEER records, empirical correlation between magnitude and intensity is proposed for the detection of alarming EQ. Further, proposed correlation is applied to three different sources of ground motion dataset namely K-NET, PEER and PESMOS in order find out to whether the ground motion is corresponding to a damaging EQ, based on P wave arrival and subsequently use the information to issue a warning in advance. In the absence of recorded ground motion for major to great EQs in India, synthetic ground motions developed in earlier work are used for identification of damaging EQs and issuing of alarm.

*Conclusions:* Overall, it is found that out of 149 EQ records ( $M \geq 5$ ) considered in this work, 139 EQs are found correct to raise warning, based on the proposed methodology. In addition, the time window of escape between issue of warning and the actual arrival of secondary waves, are found to vary from 0s to 1mins approximately. Findings from present work concludes that identification of damaging EQ based on first 3s P wave signature, as followed in US and Japan are also compatible for Indian subcontinent towards development of a EEW for the country. This will be very helpful in minimizing casualties and building damages during probable future EQs in India.

**Keywords:** Earthquake early warning, compact UrEDAS, destructive intensity, isoseismal maps, time window

## 1 Introduction

Earthquake (EQ) is a form of natural hazard which is unpredictable and independent of the terrain type. This nature of EQ makes it a dominant form of natural hazard that can inflict equal harm upon human beings and infrastructure almost everywhere across the globe. With rapid increase in human population and haphazard urbanization, especially in the developing countries, the dangers from EQs have increased many folds compared to the past. Hence, studies have been conducted to develop methods that can help to mitigate the risks during future EQs. One such method is the Earthquake Early Warning (EEW) which can detect an EQ occurrence in real time and trigger alarms to the nearby localities and to distant regions as well before the actual arrival of secondary waves at the site; thus, giving a possible time window for escape and minimizing the loss of lives. The basic work principle of an

---

\* Corresponding Author

EEW system involves the detection of the arrival of first seismic wave generated by an EQ at the recording stations. Based on a threshold value of the selected parameter (magnitude or intensity) in that particular EEW system, a warning will be issued to the target site (e.g. a densely populated city or railway station). Thus, before the actual arrival of the damage causing secondary waves at that particular site, people will be prepared in advance. Hence, the time interval between the issue of alarms and the arrival of secondary waves at the site can be used for mitigation and transfer of the population to safer locations. Since, the warning is issued earlier to the actual arrival of damage causing secondary wave, such systems are called as Earthquake Early Warning (EEW) systems. There are two approaches to the EEW system namely regional EEW and on-site EEW. In the regional EEW system, a number of seismic sensors, in the form of an array are placed around the possible regions of EQ occurrence. These seismic sensors detect the arrival of the P wave and if found potential, an alarm is issued. In case of on-site EEW system, the seismic sensors are placed at the target site itself. Hence, on the arrival of a P wave at the target site from a potentially damaging EQ, the alarm is issued before the arrival of the secondary wave.

## 2 Background

### 2.1 EEW System Worldwide

Issuing early warnings in the real time, an EEW system uses computerized seismic stations that provide fast and reliable information about an EQ event such as location, time and size of the EQ along with the recorded ground motions. EEW systems are operational in various countries across the globe. Some of these systems include; Seismic Alert System (SAS) in Mexico City [10], UrEDAS and Compact UrEDAS in Japan [20], EEW system in Taiwan [15] and Istanbul Earthquake Rapid Response and Early Warning System (IERREWS) in Istanbul [9]. Prior to the installation of the SAS system, Mexico City was hit by an EQ of magnitude 8.0( $M_w$ ) on 19<sup>th</sup> September 1985, causing more than 10,000 casualties with more than 30,000 people injured. In order to prevent such massive disasters in the future, the SAS system was developed in 1988 and became operational since 1991 in Mexico. During the year 1995, the city of Mexico was again hit by an EQ ( $M_w$ -7.3). This time the SAS system installed in Mexico City provided a warning to the people of Copala, Guerrero through television and radio. This warning was provided almost 72s in advance before the arrival of the secondary waves in the town of Copala, Guerrero [10]. As a result of this advance warning, the residents got ample amount of time to evacuate the buildings and move to the safer places. In Guerrero region, the 1995 Mexico EQ caused extensive damage to the buildings and an intensity of VII on the MMI scale was reported. However, due to advance warning issued, the number of casualties was drastically reduced to three [27] during the 1995 Mexico EQ. Thus, the SAS system was proven to be effective towards minimizing the loss of lives during the 1995 Mexico EQ.

In another case study in Japan, the EEW system of Compact UrEDAS prevented the overturning of the Shinkansen train Toki #325 during the 2004 Niigata-ken Chuetsu EQ ( $M_w$ -6.6). The EQ had occurred on 23<sup>rd</sup> October, killing approximately 40 people while more than a thousand people were injured along with severe damages to a number of buildings [28]. This EQ had also triggered about 1300 landslides, fires at several locations and damaged numerous roads, bridges and railway lines. The shaking from the EQ was felt across Chiba, Fukushima, Gumma, Kanagawa, Miyagi, Saitama and Tokyo prefectures of Japan [28]. Considering the moderate to high intensity of shaking and reported damage to the railway lines and bridges during this EQ, the high speed Shinkansen train Toki #325, in the absence of Compact UrEDAS, might have faced a disaster similar to the high speed train derailment in Eschede, Germany in 1998 which killed about 101 people [16]. However, the effectiveness of Compact UrEDAS can be understood from the fact that the alarm based on P wave had cut off the power supply to the high speed train about 3.5s before the arrival of the secondary waves at the train location. This initiated the automatic braking system of the train and prevented the train from overturning [20]. In addition, during the time of the 2004 Niigata-ken Chuetsu EQ, EEW systems in Japan were not disseminated publically and were confined only to certain agencies. This might be a possible reason that caused moderate casualties from other locations during this EQ. With the advancement in the communication systems in Japan, it has now become much easier to warn the general public about an

incoming EQ in real time compared to 2004. Example includes the 2011 Tohoku EQ ( $M_w$ -9.0), in Japan. The origin of this EQ was located about 70km offshore towards the east of Tohoku at a focal depth of 30km in the Pacific Ocean. This EQ is considered to be the most powerful EQ ever recorded in Japan. The event had triggered Tsunami waves up to 40m in height along the coast of Tohoku and had resulted in massive ground failures such as liquefaction and differential settlements at many places [24]. This EQ had caused more than 16,000 casualties with an insured loss of over \$35 billion for Japan [23]. The above discussion clearly indicates the kind of damages and the extent of economic loss and casualties during the 2011 Tohoku EQ. Among these massive damages reported in Japan, there also exists a classical example about the role of EEW in minimizing the damaging effect of EQ in terms of human lives saved. The dissemination of the EEW system was first publicized in Japan in the year 2007 which was first tested during the 2011 Tohoku EQ. Literature exists where people staying in the city of Sendai got the EQ warnings in the form of message alerts on their cell phones. This had provided a time window of 5s before the actual ground started to shake [21]. As a consequence of this, many people could save their lives as they could run from their buildings to safer places. Even though Tsunami had hit Sendai city, the people were saved because of message alerts. The above example clearly states the role of the EEW systems in saving several lives at the same location where a high level of catastrophe had occurred. Above discussion clearly highlights that the EEW systems developed in different parts of the globe have proven their effectiveness towards minimizing the EQ induced damage scenario significantly.

Any EEW system in general is developed based on combined data of past reported EQs and the ground motion parameters. EQ recording has started only a couple of decades ago in different parts of the world. For developing countries like India, EQ records are less compared to developed countries. With limited recorded data available for any region, no EEW system is completely flawless. Hence, there are chances of missing the detection of a major EQ or raising of a wrong alarm. However, continuous efforts are being made worldwide in order to develop more efficient EEW systems so that catastrophic loss of human lives lost can be minimized.

## 2.2 EEW System for India

Indian subcontinent has a widely scattered seismicity based on EQ occurrences as well as associated damages. Regions with minimal seismicity are confined to the southern and central parts of the country. Most seismically active regions of the country on the other hand, extend towards the northern, eastern and the western parts of the Indian subcontinent. The Himalayan boundary towards the north of the country came into existence due to the collision of the Indian plate and the Eurasian plate with the Indian plate subducting. The collision started around 50 million years ago and even at present, the rate of collision is approximately 20mm/year. As a result of this, an alarming seismicity has been evidenced in the Himalayas since prehistoric times. These include EQ events in 844, 1100, 1255, 1344, 1408, 1505, 1555, 1678, 1747, 1833, 1897, 1905, 1934 and 1950. The collision had also triggered landslides at numerous locations [25]. Compared to the other parts of the country, the seismic activity of the Himalayas is much more alarming. To prevent such damages from occurring due to future EQ in the region, an EEW system could be setup to warn about an incoming EQ. Efforts are being made in this direction by the Indian Institute of Technology (IIT) Roorkee and the Ministry of Earth Sciences, Government of India [3]. IIT Roorkee proposed to install a network of 100 sensors in the Garhwal Himalayas covering an area of approximately 100km x 40km. The sensors used by IIT Roorkee were P-alert MEMS sensors which can issue an alarm within 3s of detection of a P wave originating from a damaging EQ [2]. With installation of EEW systems in India, IIT Roorkee had tested the applicability of the ground-motion period parameter  $\tau_c$  and the vertical displacement amplitude parameter  $Pd$  approach of Wu and Kanamori, [34] for Indian EQs [20]. The above program is under development.

With no EEW system in operation at present, this work is an attempt where the intensity of an EQ is considered as a new attribute for EEW systems with a special emphasis on the Himalayan EQs. The principle of Compact UrEDAS system of Japan [20] which is an on-site EEW system has been adopted. However, in this study, the principal of Compact UrEDAS has been tested for regional EEW systems and not on-site EEW. It is due to the fact that major to great EQs originating in the Himalayas had caused severe ground shaking in the densely populated regions located at considerable distance from the EQ source. Such damages were also evidenced during the 2015 Nepal EQ, even though this EQ had

originated in the Himalayas the shaking was felt 1000km away in Delhi. Hence, the use of a regional EEW system would be more effective for EQs in the Himalayas. The principle of Compact UrEDAS is also adopted since it can derive the destructiveness of an EQ in real time directly from the EQ motion without wasting crucial time on analyzing EQ parameters such as predominant frequency or V/H ratio as done in other EEW systems.

### 3 Method

Compact UrEDAS was derived from UrEDAS (Urgent Earthquake Detection and Alarm System). The idea of UrEDAS was proposed by Nakamura, [32]. As per Nakamura, [32], UrEDAS uses magnitude and location parameters of an EQ to measure its strength and issues an alarm accordingly. UrEDAS requires a processing time of 3s to issue a warning after detecting the arrival of P wave generated due to an EQ. As per Nakamura et al. [33], after the 1995 Kobe EQ, a new system was developed to reduce the processing time to 1s after the detection of the arrival of P wave. This new system was called as the Compact UrEDAS. Both UrEDAS and Compact UrEDAS were designed to issue alarm to the high speed trains in Japan. When the alarms trigger based on P wave detection, the automatic braking system of the trains initiate and stop the trains before the arrival of the secondary waves. For this reason, both UrEDAS and Compact UrEDAS are mostly installed along the high speed railway lines of Japan. As per Frances and Daniel [12], a total of 56 Compact UrEDAS were installed along the Shinkansen line in 1997. In the later years, more Compact UrEDAS were installed along the Tohoku, Joetsu, and Nagano Shinkansen Lines and also along the Tokyo subway system [12]. The Compact UrEDAS was tested successfully in real time during the Sanriku-Minami EQ (Mw-7.0). This EQ had occurred on 26<sup>th</sup> May 2003 near the east coast of the Honshu Island of Japan. According to Frances and Daniel [12], the Compact UrEDAS systems installed along the Tohoku Shinkansen line issued the P wave alarm 1s after the detection of the P wave arrival from the EQ. Two of the high speed trains Yamabiko #59 and Hayate #26 which were running at the time of the EQ were duly alerted and stopped. As a consequence, it prevented both the above mentioned trains from reaching the area that had faced the highest damages occurred during this EQ. Similarly, during the 23<sup>rd</sup> October 2004 Niigata-ken Chuetsu EQ(Mw-6.6), the Compact UrEDAS performed effectively to stop the high speed Shinkansen train Toki #325 before it could reach the area hit very badly by the EQ [20].

From above practical applications of the Compact UrEDAS, it can be observed that the issue of the P wave alarm within 1s of the P wave arrival is very effective. Significant reduction in the processing time to issue an alarm in Compact UrEDAS, compared to its predecessor has considerably enhanced its effectiveness. A Compact UrEDAS does not estimate EQ parameters such as magnitude and location to detect if it is a damaging EQ. Instead Compact UrEDAS quantifies the strength of an EQ in terms of Destructive Intensity (DI) in real-time and issues alarm if found potential for damages. This DI can be calculated using the equation below [30];

$$DI = \log|a \cdot v| \quad (1)$$

where, DI is the Destructive Intensity, “ $v$ ” is the velocity vector and “ $a$ ” is the acceleration vector at the recording station. Once the seismograph detects the P wave arrival, the value of DI starts increasing drastically. The peak value of DI achieved within “ $t$ ”s since P wave arrival is used as the P wave alarm. Further increase in DI values would take place at slower rates. When the S wave arrives, DI reaches its maximum value. Work performed by Nakamura [31] proposed a relation between the maximum value of DI and the Modified Mercalli Intensity (MMI) as given in Eq. (2). Similar correlation was also highlighted by Richter, (1958); Bolt [6] and Wald et al. [8].

$$MMI = (11/7)DI + 4.27 \quad (2)$$

where, MMI is the Modified Mercalli Intensity and DI is the maximum value of Destructive Intensity given by Eq. (1). Above correlation relates the maximum value of DI based on S wave with the MMI value. In the present work however, the maximum value of DI is obtained from P wave arrival. This maximum value has been called as  $DI_{max}$  in the present analyses instead of DI as given in Eq. (2).

## 4 Results

### 4.1 Data and Analysis

National Research Institute for Earth Science and Disaster Prevention (NIED) in Japan installed K-NET strong motion network. The term K-NET stands for ‘Kyoshin NETwork’ where ‘Kyoshin’ means ‘strong motion’ in Japanese. The K-NET array uniformly covers the entire Japan with 1030 seismic stations whose average distance between successive stations is about 20km. These seismic stations record the EQ shaking at a sampling rate of 100Hz (K-NET). Since, the principal of Compact UrEDAS system developed for Japan, which is used in the present work, the ground motion records from K-NET are considered first for the analyses. Records of 21 EQs from K-NET with a magnitude range of 5.0 to 7.3 and within epicentral distance less than 70km are considered. This range of epicentral distance is considered here keeping in mind the very limited data within the epicentral region (<50km) available in PESMOS database for the Himalayas which is the area under consideration in this work. Further increase in the range of epicentral distance will have a direct impact on the processing time and subsequent delay in issuing the alarm, which might not be desirable for the present objective.

For each of the EQ records selected above, the arrival time of the P wave at the seismic station is estimated. Further, the Destructive Intensity (DI) value for each of the EQ records is estimated as per Eq. (1). This involves integrating the acceleration time history using MATLAB code to determine the velocity records. Further, using MATLAB code, obtained velocity records are filtered with a high-pass Butterworth filter with a cut-off frequency of 0.075Hz to separate the noise. It has to be mentioned here that when a seismic sensor records an EQ, along with it low frequency noise also gets recorded. This noise could severely affect the process of detection of damaging EQs. Hence, a high-pass Butterworth filter is used to remove the low frequency noise. The high-pass Butterworth filter of 0.075Hz is used in reference to past studies such as Wu and Kanamori [34], Böse et al. [13] and Bhardwaj et al. [20]. Thus, the velocity vector obtained is multiplied with the acceleration vector. The maximum value of the product of acceleration vector and velocity vector since the first P wave arrival at the sensor is taken as the  $DI_{max}$  value for each EQ records. Wu and Kanamori, [34] had used the first 3s of secondary wave to determine its size. A similar time window of 3s is adopted in the present work to determine the DI value since the arrival of P wave. It has to be mentioned here that for EEW systems time is the most crucial factor, due to which early warning systems such as the UrEDAS take the minimum time of 3s to measure the strength of an earthquake event and issue a warning. More advanced EEW systems such as the on-site Compact UrEDAS require even less processing time of 1s. A longer processing time may provide more accurate results and reduce the chances of a false alarm. However, a longer processing time also reduces the time window for issuing an alarm before the arrival of the S-wave at the target site. It has been mentioned earlier that according to Kumar et al. [2] the P-alert MEMS sensors used for Indian EQs can issue an alarm within 3s of detection of a P wave. As this study is conducted for Indian scenario and applies the principle of Compact UrEDAS for a regional EEW systems rather than on-site EEW system, the 3s processing time is found applicable in the present work. Based on the present analysis, it is found that the value of DI starts to increase after the P wave arrival similar to the findings of Nakamura et al. [33]. This indicates that the value of DI is sensitive to the detection of the P wave. Further, the  $DI_{max}$  value obtained within a time window of 3s from P wave arrival is used as the P wave alarm. This  $DI_{max}$  value indicates the damaging power of an EQ similar to the intensity scale, hence it is compared with the MMI scale as per Eq. (2). Since the  $DI_{max}$  values and the subsequent MMI values estimated as per Eq. (1) and (2) are based on P wave arrival, the MMI obtained has been named as MI-P known as Modified Intensity for P wave alarm (MI-P) in the present work. This new parameter is an indicator of destructiveness of the EQ as evaluated from  $DI_{max}$  value from the P wave of the EQ records.

Further, a linear regression is performed between the magnitude (M) of the EQ and the MI-P values. All the 21 EQs records from K-NET are used for the regression. It has to be mentioned here that only the average MI-P value for each EQ obtained from four recording stations closest to the epicenter within 70km is used. This has been done to obtain the optimum relation between M and MI-P. The average MI-P is referred as  $(MI-P)_{av}$  from here onwards in this paper. Based on least square approach, the

following functional form between  $(MI-P)_{av}$  and  $M$  is obtained. It has to be mentioned that no other functional form is existing at present between these two parameters.

$$(MI - P)_{av} = 1.17M - 1.86 \quad (3)$$

where,  $(MI-P)_{av}$  is the average MI-P value for the four stations closest to the epicenter located within 70km and  $M$  is the magnitude of the EQ. Figure 1 shows regression between the  $(MI-P)_{av}$  and magnitude ( $M$ ) values along with the K-NET dataset used in the linear regression. It can be observed from the Figure 1 that both the values of  $(MI-P)_{av}$  and  $M$  show strong correlation. Further, this correlation is applicable for the magnitude range of 5.0 to 7.3. It has to be highlighted here that each point in Figure 1 represents the average value of 4 stations. Further, considering Eq. (3) the threshold values 6.0 for magnitude is set to issue an alarm. This value of magnitude is selected since the lower values of magnitude do not cause considerable damages to the buildings and other infrastructure. Considering a magnitude value of 6, the corresponding  $(MI-P)_{av}$  value as 5.15 is obtained as per Eq. (3).

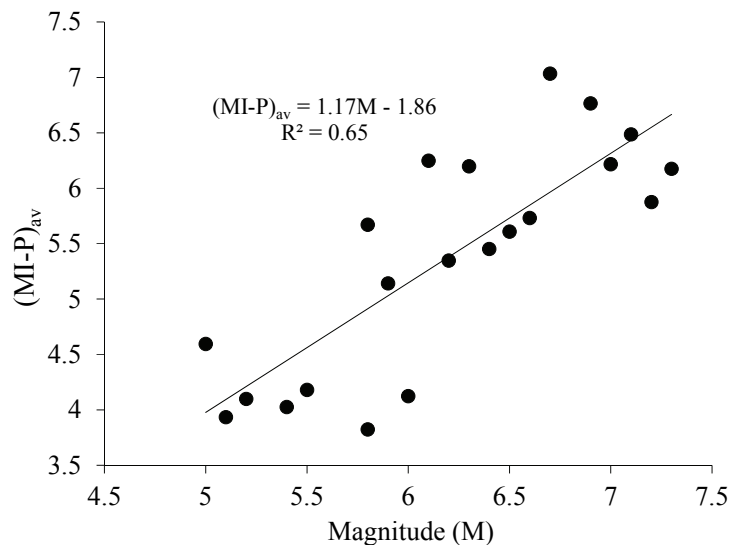


**Figure 1.** Regression of MI-P with magnitude ( $M$ )

## 4.2 Validation of Proposed Correlation

In order to check the effectiveness of the above proposed correlation in terms of detecting a true alarm and subsequently issuing a warning, validation has been done for other databases. EQ records from K-NET, PESMOS and PEER with magnitude  $\geq 6.0$  are considered. PESMOS (Program for Excellence in Strong Motion Studies) is the database of strong ground motions recorded by the Indian Strong Motion Instrumentation Networks (<http://pesmos.in>). PESMOS is operated by Earthquake Engineering Department, IIT Roorkee, India. The recording stations of the Indian Strong Motion Instrumentation Networks are spread throughout the Himalayan belt from Jammu and Kashmir in the west to Meghalaya in the east. The entire network consists of more than 250 stations. PEER (Pacific Earthquake Engineering Research, <http://peer.berkeley.edu/smcat/sites.html>) is operated by NISEE (National Information Service for Earthquake Engineering) at University of California, Berkeley. The PEER strong motion database contains acceleration, velocity and displacement time histories of EQs. Further, it also provides response spectra at several percentages of damping levels. Information about the magnitude, site characterization, peak values etc. is also available [5]. Ground motion recording in India was started only after 1986 and since then not many major EQs have occurred. Thus, the database from PESMOS will have very limited ground motion records from major to great EQs which had caused considerable damages in the Himalayas. Existing gap in the available ground motion database in terms of entire range of hypocentral distance as well as for higher magnitudes in the Himalayan region was highlighted by Anbazhagan et al. [19]. This gap was filled by generating synthetic ground motions for 14 selected EQs which had occurred at different segments of the Himalayan belt by Anbazhagan et al. [19]. For each EQ, 30 synthetic ground motions were generated after considerable

validation of various ground motion model parameters. For historic EQs with no ground motion records available, published isoseismal maps were utilized to understand the level of ground shaking during each of the EQ event. Finally a new ground motion prediction equation (GMPE) was developed by Anbazhagan et al. [19] by combining both the recorded as well as synthetic ground motions. Sufficient validation of the above synthetic ground motions referred above in terms of acceleration time history, Fourier spectra and response spectra at bedrock was presented by Anbazhagan et al. [19] and has not been reproduced here. In the present work, continuing with the limitation of PESMOS database for major to great EQ records, synthetic ground motions developed by Anbazhagan et al. [19] are utilized. Thus, the combined databases (PESMOS + synthetic ground motions) cover a wide range of EQ records and will be very helpful in checking the effectiveness of the proposed principle for the Himalayas. To validate the proposed methodology, three databases are considered in this work; K-NET, PEER and PESMOS + synthetic ground motions. Each of the selected strong motion records are corresponding to magnitude  $\geq 6$ . The data from the above mentioned sources consist of different magnitude scales and thus, no specific magnitude scale is considered in this work. It has to be highlighted here the outcome of this work is to provide qualitative information in terms of *alarm*, any change in the magnitude scale will not affect the issuing of alarm considerably. As highlighted earlier, ground motion records should be recorded within the epicentral distance of 70km to be used in the present work.

For each of the database namely K-NET, PEER and PESMOS + synthetic ground motions, the plots between MI-P and M are obtained. Each of the plots is further divided into 4 quadrants. The first quadrant consists of the records exceeding both the threshold values (magnitude as well as MI-P) and thus “*True alarm*” is issued for these records. “*False alarm*” is issued for the records in the second quadrant, which are of  $M < 6$  i.e. not damaging EQs but exceed the MI-P threshold value. The third quadrant consists of records with  $M < 6$  and  $MI-P < 5.15$  for which “*Correct no alarm*” is issued. The records in the fourth quadrant exceed the threshold value of M but not MI-P; it is a case of “*Missed alarm*” where a damaging EQ remained undetected.

In the first attempt, a total of 57 EQ records from K-NET with a magnitude range of 5.0 to 7.3 are analyzed. Figure 2 shows the MI-P versus M variation for K-NET data. It can be observed from Figure 2 that out of a total of 57 records, 40 records are found as *True Alarms* while *Correct no Alarm* has been detected for 14 records. The number of *False alarm* and *Missed Alarm* are found as 2 and 1 respectively. Thus, based on the analysis, only 2 *False Alarms* are found out of a total 57 records. Summary about each quadrant for K-NET record is presented in Table 1.

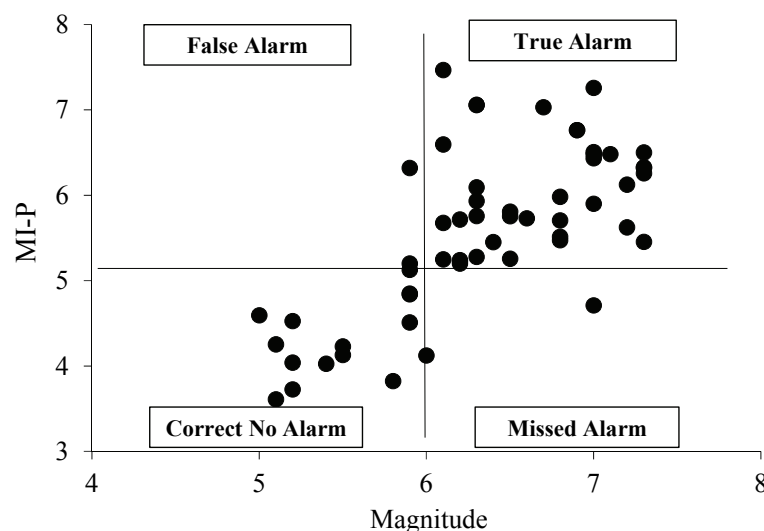
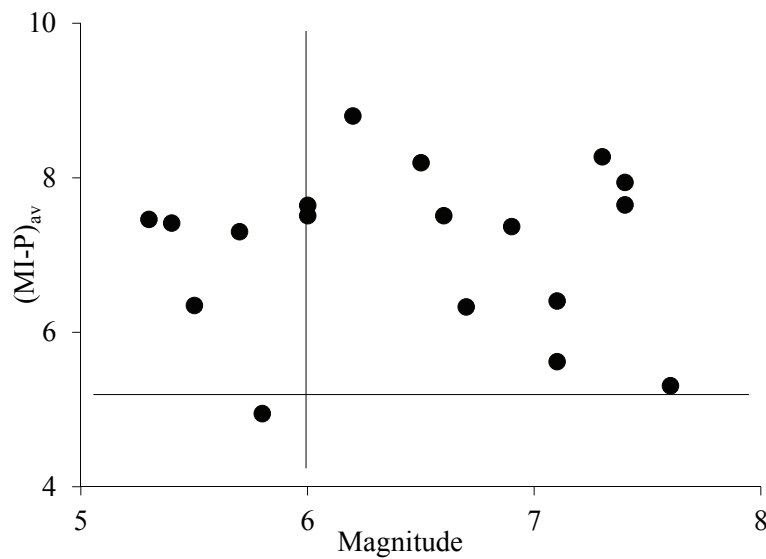


Figure 2. P wave alarm plot for K-NET records

**Table 1.** P wave alarms issued for K-NET records

S. NO.	Alarm type	Number of alarms
1.	True alarm	40
2.	False alarm	2
3.	Correct no alarm	14
4.	Missed alarm	1

Again, similar analysis is attempted considering PEER data. A total of 46 EQ records in the magnitude range of 5.3 to 7.6 are considered as shown in Figure 3. Out of 46 records, a total of 12 records are detected as *Missed alarm*. Remaining 34 records consists of 29, 1 and 4 number of *True alarm*, *Correct no alarm* and *False Alarms* respectively. Summary about each quadrant for PEER records is presented in Table 2.

**Figure 3.** P wave alarm plot for PEER records**Table 2.** P wave alarms issued from PEER records

S. NO.	Alarm type	Number of alarms
1.	True alarm	29
2.	False alarm	4
3.	Correct no alarm	1
4.	Missed alarm	12

Based on the summary, it can be said that in case of PEER database as well, *False Alarm* is very low similar to the findings from K-NET records. In order to further reduce the number of *Missed alarm*, average records from four stations close to the epicenter are taken in case of PEER record and MI-P versus M are plotted as shown in Figure 4. It can be observed from Figure 4 that in comparison to Figure 3, the number of *Missed Alarm* has reduced considerably in Figure 4. Summary about each quadrant for average PEER records is presented in Table 3 with no *Missed Alarms*.

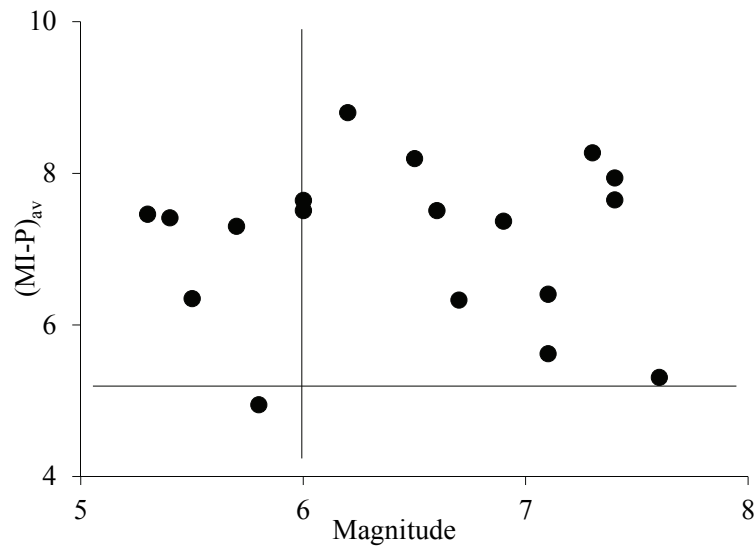


Figure 4. M versus average MI-P value plot for averaged PEER records

Table 3. P wave alarms issued from average PEER records

S. NO.	Alarm type	Number of alarms
1.	True alarm	13
2.	False alarm	4
3.	Correct no alarm	1
4.	Missed alarm	0

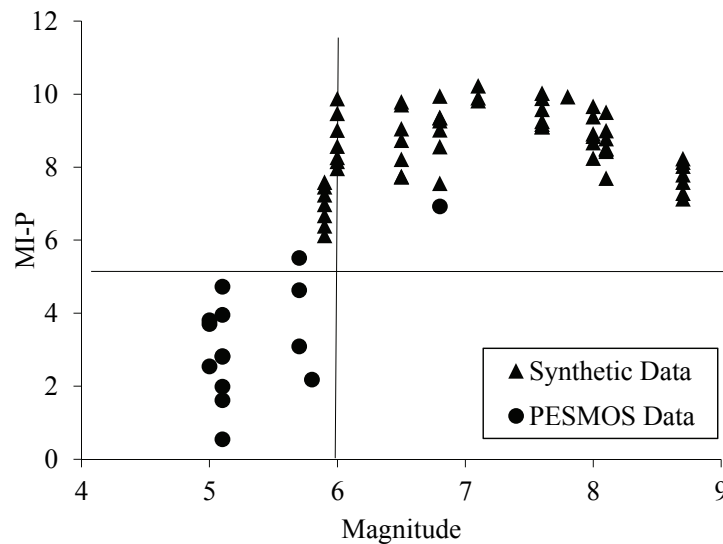


Figure 5. P wave alarm plot for PESMOS+ synthetically generated records

PESMOS database consists of ground motion records based on arrays of seismic recording stations such as Kangra array, Uttar Pradesh array and the Sikkim array. It provides the largest catalogue of the ground motion records in India. The database consists of ground motion records since 2005. In order to check the effectiveness of MI-P parameter in detecting *True* and *False alarm*, ground motion records from PESMOS are also attempted. Ground motion records from PESMOS do not contain records of higher magnitude EQ ( $M \geq 6.8$ ). In order to check the effectiveness of the proposed principle for major

to great EQs in the Himalayas, synthetic ground motions from Anbazhagan et al. [19] are considered for magnitude range of 5.9 to 8.7. Plot of MI-P versus magnitude based on PESMOS + synthetic ground motions is presented in Figure 5.

A total of 15 records from PESMOS and 59 synthetic ground motion records are analyzed. It can be observed from Figure 5 that in case of PESMOS records; only one ground motion has magnitude greater than 6.0 which has been detected as *True Alarm*. Remaining records consists of 1 *False Alarm* while 13 records having magnitude less than 6.0 and the MI-P less than 5.15 are detected as *Correct no Alarm*. It has to be highlighted here that no record has been detected as *Missed Alarm* based on PESMOS database. Further, considering synthetic ground motion records, out of a total of 59 records, 52 records are detected as *True Alarms*. The numbers of *False alarms* detected are 7 with no *Missed Alarm* or *Correct no Alarm*. Summary about each quadrant for PEMOS and synthetically generated records can be obtained from Table 4.

**Table 4.** P wave alarms issued for PEMOS + synthetically ground motion records

S. NO.	Alarm type	Number of alarms
1.	True alarm	53
2.	False alarm	8
3.	Correct no alarm	13
4.	Missed alarm	0

From the above analyses, the effectiveness of the proposed correlation to detect an EQ is checked for K-NET, PEER and PESMOS database. In order to check the applicability of proposed correlation for higher magnitudes ( $M > 6.8$ ), synthetic ground motion records are also used. Based on the above validation, it is found that for 149 EQ records 139 alarms were correctly issued. Further, the usefulness of the proposed correlation is checked for case studies related to three damaging EQs in the Himalayas in the later section.

## 5 Discussions Based on Case Studies for Three Major to Great Earthquakes in the Himalayas

The effectiveness of adopted methodology of Compact UrEDAS for the Himalayas is further validated in this section. The MI-P values obtained from the above principle are compared with the reported MMI values for major to great EQs with no ground motion records in the Himalayas. Three EQs used for validation purpose in the present work include; the 1905 Kangra EQ (M-7.8), the 1934 Bihar-Nepal EQ (M-8.1) and the 1950 Assam EQ (M-8.7). The isoseismal maps for the above EQs are obtained as per Kayal [11]. For each EQ, MI-P values are estimated using synthetic ground motion records from Anbazhagan et al., [19] for stations within an epicentral distance of 70km. Further, the reported MMI values are obtained from the isoseismal map of each EQ at the same station locations. Tables 5, 6 and 7 present comparison between the MI-P and MMI values for the 1905 Kangra EQ, 1934 Bihar-Nepal EQ and 1950 Assam EQ respectively.

**Table 5.** MMI values for 1905 Kangra earthquake (Mw=7.8)

Station name	Station coordinate		Epicentral distance (km)	MMI based on	
	Latitude	Longitude		Isoseismal map	MI-P
1	32.70N	76.90E	10	9	11
2	32.80N	77.00E	20	8	10
3	33.00N	76.80E	30	8	10
4	33.10N	76.80E	40	8	10
5	33.20N	76.60E	50	8	10
6	33.30N	76.40E	60	8	10
7	33.30N	76.20E	70	7	9

**Table 6.** MMI values for 1934 Bihar-Nepal earthquake (Mw=8.1)

Station name	Station coordinate		Epicentral distance (km)	MMI based on	
	Latitude	Longitude		Isoseismal map	MI-P
1	26.70N	87.10E	10	9	11
2	26.90N	87.10E	20	9	10
3	27.00N	87.10E	30	9	9
4	27.10N	87.10E	40	9	9
5	27.20N	87.00E	50	9	9
6	27.30N	86.60E	60	8	9
7	27.40N	86.60E	70	8	8

**Table 7.** MMI values for 1950 Assam earthquake (Mw=8.7)

Station name	Station coordinate		Epicentral distance (km)	MMI based on	
	Latitude	Longitude		Isoseismal map	MI-P
1	28.40N	95.00E	10	10	8
2	28.60N	95.00E	20	9	8
3	28.70N	95.00E	30	9	8

It can be observed from Table 5 that both sets of values (MI-P and MMI) are closely matching for the 1905 Kangra EQ up to epicentral distance of 70km. It has to be highlighted here that the MMI values are based on reported damages while the MI-P values are based on ground motion records. Similar matching between the two sets of intensities can be made from Tables 6 and 7 for 1934 Bihar-Nepal EQ and 1950 Assam EQ respectively. Thus collectively it can be seen that the MMI values obtained from the isoseismal maps are very close to the MI-P values obtained using the principle of Compact UrEDAS. In addition, it can be concluded that the MI-P values obtained in this work are a correct indication of the intensity of shaking due to an EQ at a particular site. Close matching between the two sets of value enhance the confidence that the principle of Compact UrEDAS can be confidently adopted to capture the damage scenario for the Himalayan EQs as considered in the present work.

Further, to understand the practical applicability of the proposed principle, the time window between the issuing of the P wave alarm based on the MI-P values and the actual arrival of the S wave at the target site are estimated for the above mentioned three EQs. Value of P wave velocity is a regional property and can vary from region to region. Singh et al. [26] proposed Artificial Neural Network (Ann) based method to determine P wave velocity of rocks as a function of chemical composition and physico-mechanical properties of rock. In another work, Verma and Singh [1] proposed empirical correlation to arrive at Peak Particle Velocity which is going to be generated during blasting. Genetic Algorithm technique is used in developing correlation based on 127 blast records from the region of Kumaria mine.

For each of these EQs in the present work however, the time of arrival of the P wave at the seismic stations is observed considering P wave velocity of 6.3km/s as listed in column 3 in Tables 8, 9 and 10. Further, a time window of 3s is added to first P wave arrival time to account for the estimation time for MI-P values as discussed earlier. Final issuing of the P wave alarm is listed in column 4 in Tables 8, 9 and 10. It has been mentioned earlier that in EEW systems, time of issuing of alarm is most crucial. Once all the stations detect the P wave arrival, arrival time from only first four of the seismic stations, placed closest to the epicenter, are taken into account out of 7 seismic stations listed in Tables 5 to 7. This will reduce the time of issuing the alarm in comparison to issuing alarm considering P wave detection at all the 7 seismic stations. Finally, the time of issuing an alarm to the public will be the maximum among the time required to issue the P wave alarm at all the four stations as listed in column 5 in Tables 8, 9 and 10. Next the arrival time of the S wave at the target sites is estimated based on average shear wave velocity in the propagation medium between the source and the target site as 3.6km/s as listed in column 6 in Tables 8, 9 and 10. The time difference between the issuing of the P wave alarm and the time of actual arrival of the S wave at the target site is the required time window. This time window will be used by the public to move to safer locations, similar to the case study of Japan as discussed earlier. The time windows of escape that would be available at each of the target

sites for the three EQs are shown in column 7 of Tables 8, 9 and 10 for the 1905 Kangra EQ, 1934 Bihar-Nepal EQ and 1950 Assam EQ respectively.

**Table 8.** Escape time window for 1905 Kangra earthquake (Mw = 7.8)

Epicentral distance (km)	Hypocentral distance (km)	Time of P wave arrival (s)	Minimum time to detect true alarm from each station (s)	Time of actual issuing of alarm based on observation from first four stations (s)	Time of S wave arrival (s)	Window for escape (s)
(1)	(2)	(3)	(4)	(5)	(6)	(7)
10	20.59	3.27	*6.27	9.96 <sup>#</sup>	5.72	0
20	26.91	4.27	*7.27	-	7.47	0
30	34.99	5.55	*8.55	-	9.72	0
40	43.86	6.96	*9.96	-	12.18	2.22
50	53.14	8.44	-	-	14.76	4.80
60	62.64	9.94	-	-	17.40	7.44
70	72.28	11.47	-	-	20.08	10.11
80	82.00	13.02	-	-	22.78	12.82
90	91.78	14.57	-	-	25.50	15.53
100	101.61	16.13	-	-	28.22	18.26
110	111.46	17.69	-	-	30.96	21.00
120	121.34	19.26	-	-	33.71	23.74
130	131.24	20.83	-	-	36.46	26.49
140	141.15	22.41	-	-	39.21	29.25
150	151.08	23.98	-	-	41.97	32.00
160	161.01	25.56	-	-	44.72	34.76
170	170.95	27.13	-	-	47.49	37.52
180	180.90	28.71	-	-	50.25	40.29
190	190.85	30.29	-	-	53.01	43.05
200	200.81	31.87	-	-	55.78	45.82
210	210.77	33.46	-	-	58.55	48.58
220	220.74	35.04	-	-	61.32	51.35
230	230.70	36.62	-	-	64.08	54.12
240	240.67	38.20	-	-	66.85	56.89

\*alarm generation time up to 40km from the epicenter have only been considered to save time

<sup>#</sup>maximum time required to issue the alarm among the four stations within 40km from the epicenter

**Table 9.** Escape time window 1934 Bihar-Nepal earthquake (Mw=8.1)

Epicentral distance (km)	Hypocentral distance (km)	Time of P wave arrival (s)	Minimum time to detect true alarm from each station (s)	Time of actual issuing of alarm based on observation from first four stations (s)	Time of S wave arrival (s)	Window for escape (s)
(1)	(2)	(3)	(4)	(5)	(6)	(7)
10	18.03	2.86	*5.86	9.78 <sup>#</sup>	5.01	0
20	25.00	3.97	*6.97	-	6.94	0
30	33.54	5.32	*8.32	-	9.32	0
40	42.72	6.78	*9.78	-	11.87	2.09
50	52.20	8.29	-	-	14.50	4.72
60	61.85	9.82	-	-	17.18	7.40
70	71.59	11.36	-	-	19.89	10.10
80	81.39	12.92	-	-	22.61	12.83
90	91.24	14.48	-	-	25.34	15.56

100	101.12	16.05	-	-	28.09	18.31
110	111.02	17.62	-	-	30.84	21.06
120	120.93	19.20	-	-	33.59	23.81
130	130.86	20.77	-	-	36.35	26.57
140	140.80	22.35	-	-	39.11	29.33
150	150.75	23.93	-	-	41.87	32.09
160	160.70	25.51	-	-	44.64	34.86
170	170.66	27.09	-	-	47.41	37.62
180	180.62	28.67	-	-	50.17	40.39
190	190.59	30.25	-	-	52.94	43.16
200	200.56	31.84	-	-	55.71	45.93
210	210.54	33.42	-	-	58.48	48.70
220	220.51	35.00	-	-	61.25	51.47
230	230.49	36.59	-	-	64.02	54.24
240	240.47	38.17	-	-	66.80	57.02

\*alarm generation time up to 40km from the epicenter have only been considered to save time

#maximum time required to issue the alarm among the four stations within 40km from the epicenter

**Table 10.** Escape time window 1950 Assam earthquake (Mw=8.7)

Epicentral distance (km)	Hypocentral distance (km)	Time of P wave arrival (s)	Minimum time to detect true alarm from each station (s)	Time of actual issuing of alarm based on observation from first four stations (s)	Time of S wave arrival (s)	Window for escape (s)
(1)	(2)	(3)	(4)	(5)	(6)	(7)
10	36.40	5.78	*8.78	11.44 <sup>#</sup>	10.11	0
20	40.31	6.40	*9.40	-	11.20	0
30	46.10	7.32	*10.32	-	12.80	1.37
40	53.15	8.44	*11.44	-	14.76	3.33
50	61.03	9.69	-	-	16.95	5.52
60	69.46	11.03	-	-	19.30	7.86
70	78.26	12.42	-	-	21.74	10.30
80	87.32	13.86	-	-	24.26	12.82
90	96.57	15.33	-	-	26.82	15.39
100	105.95	16.82	-	-	29.43	17.99
110	115.43	18.32	-	-	32.06	20.63
120	125.00	19.84	-	-	34.72	23.29
130	134.63	21.37	-	-	37.40	25.96
140	144.31	22.91	-	-	40.09	28.65
150	154.03	24.45	-	-	42.79	31.35
160	163.78	26.00	-	-	45.50	34.06
170	173.57	27.55	-	-	48.21	36.78
180	183.37	29.11	-	-	50.94	39.50
190	193.20	30.67	-	-	53.67	42.23
200	203.04	32.23	-	-	56.40	44.96
210	212.90	33.79	-	-	59.14	47.70
220	222.77	35.36	-	-	61.88	50.44
230	232.65	36.93	-	-	64.62	53.19
240	242.54	38.50	-	-	67.37	55.94

\*alarm generation time up to 40km from the epicenter have only been considered to save time.

#maximum time required to issue the alarm among the four stations within 40km from the epicenter

The three EQs considered above, for generation of time windows for escape are among the most damaging EQs of India. As per Thakur et al. [29], the impact of the 1905 Kangra EQ (M-7.8) was felt

over 300km from Kangra to Mandi and Kullu towards east to Dehradun in the south. The EQ caused severe damages with approximately 20,000 casualties. In light of the time window of escape estimated for this particular EQ (ref to Table 8), it can be said that a number of lives could have been saved. From the Table 8, it can be seen that the P wave alarm is issued at a maximum time of 9.96s since EQ occurrence. With respect to issue of alarm, a considerably larger time window of 56.89s is available for the station located at 240km from the epicenter. In scenarios such as the 1905 Kangra EQ where the damages had extended up to 300km, a time window of close to a minute at a distance of 240km can be very effective in saving many human lives.

Similarly, for the case of the 1934 Bihar-Nepal EQ ( $M=8.1$ ), the longest time window of 57.02s is available at 240km from the epicenter (refer Table 9). The 1934 Bihar-Nepal EQ is considered as one of the great EQs in India which had caused wide spread damages causing more than 10,000 casualties. Further, this EQ had caused wide spread liquefaction and damage in India and adjoining regions [4]. In Nepal, at several locations, the ground had slumped, tilted and fissured. The entire area south of the Nepal border was called as 'The Slump Belt' by Pandey and Molnar [14]. The Slump Belt had extended over a distance of 300km. Since the shaking from the EQ was felt across several hundreds of kilometers, issuing of the P wave alarm within a minimum time of 9.78s can provide sufficient window for escape, at several locations.

Another great EQ of India was the 1950 Assam EQ ( $M=8.7$ ). This EQ had caused damages in both Tibet and in the northeastern India. It also caused ground fissures at several places [18], [17]. Ground shaking due to this EQ was felt up to Kolkata, West Bengal [7] which is located at approximately 1500km from the epicenter of the EQ. At a distance of 240km for this EQ, an escape window of 55.94s is obtained as shown in column 8, Table 10 which can be used effectively to escape during the EQ. It has to be highlighted here that the time window for escape at the target sites closest to the epicenter is almost negligible. This is due to fact that the time difference between the arrival of S wave and issue of alarm will not be significant. As the epicentral distance increases, the time difference between the issue of alarm and the arrival of S wave will increase and hence the issuing of the P wave alarm becomes more effective.

## 6 Conclusions

The Himalayan seismicity has been an alarming threat to the nearby as well as distant locations. Moderate to complete damages during past EQs are well documented for the Himalayan. EEW systems have proven very effective in terms of minimizing the casualties during an EQ, in different parts of the globe as discussed earlier. However, such systems are rarely available in India at present. In this study, the intensity of EQ has been used as an attribute for EEW system to detect damaging EQs. The DI approach of Compact UrEDAS is adopted in this work to test intensity as an attribute using the K-NET [22] database. The  $DI_{max}$  values obtained within a time window of 3s after the arrival of the P wave at the seismic station are estimated and then compared to the MMI scale. Since the MMI values obtained are only from the P wave part of the EQ waves, these are termed as MI-P values. A linear regression is performed between the magnitude ( $M$ ) and the MI-P values to set threshold values of magnitude 6 and corresponding MI-P value of 5.15 for detection of damaging EQs. Ground motion records exceeding these threshold limits are recognized as damaging EQs. The effectiveness of the proposed MI-P in order to detect alarms is tested for K-NET [22], PEER and PESMOS database. Avoiding the limitation of recorded ground motions for larger magnitude in PESMOS, synthetic ground motion records up to magnitude of 8.7 are also tested for the proposed correlation. Based on the analyses, it is found that significantly large portion of *True alarms* are detected from all the databases. Overall, out of 149 EQ records, detection for 139 EQ records is found correct.

To further validate the usefulness of present analyses for Indian EQs, the MI-P values obtained are compared to MMI values during the 1905 Kangra EQ, the 1934 Bihar-Nepal EQ and the 1950 Assam EQ. Analyses found that the MI-P values obtained for above EQs using synthetic ground motions are matching closely with the MMI values obtained from the isoseismal map at numerous locations considered. Further, to understand the practical applicability of the proposed idea, the time window between the issuing of the P wave alarm based on the MI-P values and the actual arrival of the S wave at the target sites are estimated. For each of the above three EQ, the time window for escape is found

to increase with distance, going up to almost a minute at approximately 240km from the epicenter. From the damage reports of these major to great EQs of India it is clear that the damages were spread across several kilometers. Sufficient time window for escape obtained using the present principle can significantly minimize damage scenario if case of issue of alarms.

## List of Abbreviations

ANN	Artificial Neural Network
DI	Destructive Intensity
$DI_{max}$	maximum value of Destructive Intensity
EEW	Earthquake Early Warning
EQ	Earthquake
GMPE	Ground Motion Prediction Equation
IERREWS	Istanbul Earthquake Rapid Response and Early Warning System
K-NET	Kyoshin NETwork
M	Magnitude
MMI	Modified Mercalli Intensity
MI-P	Modified Intensity for P wave alarm
$(MI-P)_{av}$	average value of Modified Intensity for P wave alarm
NIED	National Research Institute for Earth Science and Disaster Prevention
NISEE	National Information Service for Earthquake Engineering
PEER	Pacific Earthquake Engineering Research
PESMOS	Program for Excellence in Strong Motion Studies
SAS	Seismic Alert System
UrEDAS	Urgent Earthquake Detection and Alarm System

## List of Symbols

$M_w$	Moment Magnitude of Earthquake
$M$	Magnitude of Earthquake
$v$	Velocity Vector
$a$	Acceleration Vector
$MI-P$	Modified Intensity for P wave alarm
$(MI-P)_{av}$	Average MI-P value
$DI$	Destructive Intensity
$DI_{max}$	Maximum Destructive Intensity
$DI_{av}$	Average Destructive Intensity

## Declarations

- Availability of data and material

The datasets analyzed during the current study are available in K-NET (Kyoshin NETwork, [www.kyoshin.bosai.go.jp](http://www.kyoshin.bosai.go.jp)), PEER (Pacific Earthquake Engineering Research, <http://peer.berkeley.edu/smcat/sites.html>) and PESMOS (Program for Excellence in Strong Motion Studies, <http://pesmos.in>). From K-NET [22] 21 ground motion records with a magnitude range of 5.0 to 7.3 and within epicentral distance less than 70km from K-NET [22] are considered. From PEER with earthquakes of magnitude  $\geq 6.0$  are considered. PEER is operated by NISEE (National Information Service for Earthquake Engineering) at University of California, Berkley. Similarly for PESMOS also earthquakes of magnitude  $\geq 6.0$  are considered is the database of strong ground motions recorded by the Indian Strong Motion Instrumentation Networks. PESMOS is operated by Earthquake Engineering Department, IIT Roorkee, India. The database from PESMOS will have very limited ground motion records from major to great EQs. This gap was filled by Anbazhagan et al. [19] by generating synthetic ground motions. In the present work, continuing with the limitation

of PESMOS database for major to great EQ records, synthetic ground motions developed by Anbazhagan et al. [19] are utilized.

- Competing interests

The authors declare that they have no competing interests.

- Authors' contributions

OB<sup>1</sup> collected the data from K-NET [22], PEER and PESMOS then analyzed and interpreted the data regarding the effectiveness of the proposed MI-P for issuing of alarms. AK<sup>2</sup> contributed substantially towards the conceptualization and drafting of the work. AK<sup>3</sup> provided the data for validation of the study in terms of three major to great earthquakes in the Himalayas. AK<sup>3</sup> also substantively revised the study.

- Acknowledgements

The authors would like to acknowledge the funding provided by the Department of Science and Technology (DST), government of India, and the Ministry of Earth Sciences (MoES) for installation of strong motion instrumentation network from which a major portion of the data used in this study has been acquired. The authors are thankful to the Department of Earthquake Engineering, Indian Institute of Technology, Roorkee and Department of Civil Engineering, Indian Institute of Technology, Guwahati for the technical support provided by both the institutions.

## References

1. A. K. Verma and T. N. Singh, "Intelligent systems for ground vibration measurement: a comparative study", *Engineering with Computers*, vol. 27, no.3, pp. 225-233, 2011.
2. A. Kumar, H. Mittal, B.P. Chamoli, A. Gairola, R.S. Jakka and A. Srivastava, "Earthquake Early Warning System for Northern India" in *Proceedings of 15<sup>th</sup> Symposium on Earthquake Engineering*, Roorkee, India, 2014.
3. A. Kumar, H. Mittal, R. Sachdeva, A. Kumar, "Indian Strong Motion Instrumentation Network", *Seismological Research Letters*, vol. 83, pp.59-66, 2012.
4. A. Kumar, N. H. Harinarayan and O. Baro, "Nonlinear soil response to ground motions during different earthquakes in Nepal, to arrive at surface response spectra", *Natural Hazards*, vol. 87, pp. 13-33, 2017.
5. B. Darragh, W. J. Silva and N. Gregor, "Strong Motion Record Processing for the PEER Center" in *Presented at Invited Workshop on Strong Motion Record Processing, 26-27 May 2004 Consortium of Organizations for Strong-Motion Observation Systems (COSMOS), Richmond, California.* (1986).
6. B.A. Bolt, "Abridged Modified Mercalli Intensity", in *Earthquakes -New Revised and Expanded Appendix C*. W.H. Freeman and Co 331, 1993.
7. CNDM, "Scenario of seismic hazard in Assam", A report by the Assam Administrative Staff College, Guwahati, Assam, India, 2012.
8. D.J. Wald, V. Quitoriano, T. H. Heaton, H. Kanamori, "Relationships between Peak Ground Acceleration, Peak Ground Velocity, and Modified Mercalli Intensity in California", *Earthquake Spectra*, vol. 15, pp. 557-564, 1999.
9. H. Alcik, O. Ozel, N. Apaydin and M. Erdik, "A study on warning algorithms for Istanbul earthquake early warning system", *Geophysical Research Letters*, vol. 36, no. 4, pp. 1-3, 2009.
10. J.M. Espinosa-Aranda, A. Cuellar, A. Garcia, G. Ibarrola, R. Islas, S. Maldonado and F.H. Rodriguez, "Evolution of the Mexican Seismic Alert System (SASMEX)", *Seismological Research Letters*, vol. 80, pp. 694-706, 2009.
11. J.R. Kayal, "Himalayan tectonic model and the great earthquakes: an appraisal", *Geomatics Natural Hazards and Risk*, vol. 1, pp. 51-67, 2010.
12. L.E. Frances, and C.G. Daniel, "Great East Japan Earthquake, JR East Mitigation Successes, and Lessons for California High-Speed Rail", MTI report, pp.12-37, 2015.
13. M. Böse, T. Heaton and E. Hauksson, "Rapid Estimation of Earthquake Source and Ground-Motion Parameters for Earthquake Early Warning Using Data from a Single Three- Component Broadband or Strong-Motion Sensor" *Bulletin of Seismological Society of America* vol. 102, no. 2, pp. 738-750, 2012.
14. M.R. Pandey and P. Molnar, "The distribution of intensity of the Bihar-Nepal earthquake of 15 January 1934 and bounds on the extent of the rupture zone" *Journal of Nepal Geological Society*, vol. 5, pp. 22-44, 1988.

15. N.C. Hsiao, Y.M. Wu, L. Zhao, D. Y. Chen, W.T. Huang, K.H. Kuo, T.C. Shin and P.H. Leu, A new prototype system for earthquake early warning in Taiwan. *Soil Dynamics and Earthquake Engineering*, vol. 31, pp. 201–208, 2011.
16. NASA, “Derailed. System Failure Case Studies”, vol. 1, no. 5, pp. 1-4, 2007.
17. O. Baro and A. Kumar, “Seismic source characterization for the Shillong plateau in northeast India. *Journal of Seismology*, vol. 21, no. 5, pp 1229–1249, 2017.
18. O. Baro. O and A. Kumar, “A review on the tectonic setting and seismic activity of the Shillong plateau in the light of past studies”, *Disaster Advances*, vol. 8, no. (7), pp. 34-45, 2015.
19. P. Anbazhagan, A. Kumar and T. G. Sitharam, “Ground motion prediction equation considering combined dataset of recorded and simulated ground motions”, *Soil Dynamics and Earthquake Engineering* vol. 53, pp. 92–108, 2013.
20. R. Bhardwaj, A. Kumar, M. L. Sharma, “Analysis of Tauc ( $\tau_c$ ) and Pd attributes for Earthquake Early Warning in India”. *Proceedings of 15<sup>th</sup> World Conference on Earthquake Engineering*, Lisboa, Portugal, 2012.
21. Seismological laboratory, Available <http://seismo.berkeley.edu/~rallen/research/WarningsInJapan>
22. Strong motion Seismograph Networks (K-NET), Available: [www.kyoshin.bosai.go.jp](http://www.kyoshin.bosai.go.jp)
23. T. H. P. Tabucchi and P. Grossi, “2011 Tohoku, Japan Earthquake Catastrophe Modeling Response”, in *Proceedings of 15<sup>th</sup> World Conference on Earthquake Engineering*, Lisboa, Portugal, 2012.
24. T. Miyagi, D. Higaki, H. Yagi, S. Doshida, N. Chiba, J. Umemura and G. Satoh, “Reconnaissance report on landslide disasters in northeast Japan following the M 9 Tōhoku earthquake” *Landslides*, vol. 8, pp.339–342, 2011.
25. T. N. Singh, A. K. Verma and K. Sarkar, “Static and dynamic analysis of a landslide”, *Geomatics Natural Hazards and Risk*, vol. 1, no. 4, pp. 323-338, 2010.
26. T. N. Singh, R. Kanchan, K. Saigal, A.K. Verma AK, “Prediction of p-wave velocity and anisotropic property of rock using artificial neural network technique”, *Journal of Scientific and Industrial Research*, vol. 63, no.1, pp. 32-38, 2004.
27. USGS, 1995 Mexico, Available: [http://earthquake.usgs.gov/earthquakes/eqarchives/significant/sig\\_1995.php](http://earthquake.usgs.gov/earthquakes/eqarchives/significant/sig_1995.php)
28. USGS, 2004 Niigata-ken Chuetsu, Available: [http://earthquake.usgs.gov/earthquakes/eqarchives/significant/sig\\_2004.php](http://earthquake.usgs.gov/earthquakes/eqarchives/significant/sig_2004.php)
29. V.C. Thakur, V. Sriram and A. K. Mundepe, “Seismotectonics of the great 1905 Kangra earthquake meizoseismal region in Kangra-Chamba, NW Himalaya”, *Tectonophysics*, vol. 326, pp. 289–98, 2000.
30. Y. Nakamura and J. Saita, “UrEDAS, the Earthquake Warning System : Today and Tomorrow In: Gasparini P., Manfredi G., Zschau J. (eds) Earthquake Early Warning Systems. Springer, Berlin, Heidelberg, 2007, pp 249-281.
31. Y. Nakamura, “On a rational strong motion index compared with other various indices”, in *Proceedings of 13<sup>th</sup> World Conference on Earthquake Engineering*, Vancouver, B.C., Canada, 2004.
32. Y. Nakamura, “On the urgent earthquake detection and alarm system (UrEDAS)”, in *Proceedings of 9<sup>th</sup> World conference on earthquake engineering*, Tokyo-Kyoto, Japan, 1988.
33. Y. Nakamura, J. Saita and T. Sato, “On an earthquake early warning system (EEW) and its applications”, *Soil Dynamics and Earthquake Engineering*, vol. 31, pp. 127–36, 2011.
34. Y. Wu and H. Kanamori, “Development of an Earthquake Early Warning System Using Real-Time Strong Motion Signals”, *Sensors*, pp. 1–9, 2008.